Journal of chemical & engineering data

Article

pubs.acs.org/jced

Thermophysical Properties of a New Dicationic Ionic Liquid

Martha Claros, Héctor R. Galleguillos, Iván Brito, and Teófilo A. Graber*

Departamento de Ingeniería Química-CICITEM, Universidad de Antofagasta, Av. Angamos 601, Antofagasta, Chile

ABSTRACT: A new functionalized dicationic ionic liquid was synthesized with the final aim of studying its application in the extraction of metal ions in the mineral industry. In light of this application, the density, refractive index, and dynamic viscosities have been determined and correlated as a function of temperature. Density data were used to calculate the volumetric properties of the ionic liquid. Several empirical equations were used to evaluate the correlation between the density and refractive indices. The results show that the modified Eykman equation has the best fit. In addition, thermal behavior was measured by thermogravimetric analysis (TGA) and differential scanning calorimetry (DSC), and a high thermal stability and a wide liquid phase range were determined.

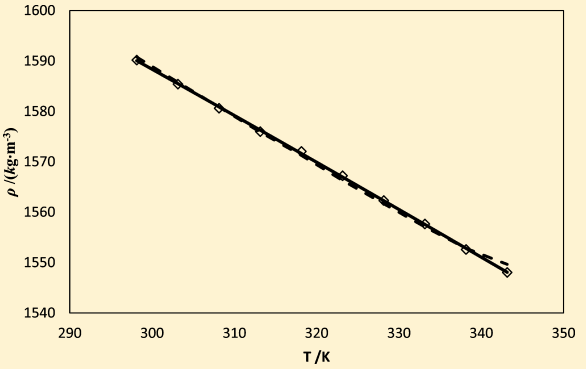

INTRODUCTION

Ionic liquids (ILs) are salts that are composed entirely of ions. They are stable in a wide range of temperature, and they have good thermal, chemical, and electrochemical stability. In addition, most have negligible vapor pressure, so there is no loss of solvent through evaporation, which avoids environmental problems due to volatilization.[1,2]

The understanding of dicationic ionic liquids (DILs), which consist of two head groups linked by a rigid or flexible spacer and two monoanions, is an interesting research topic because the numbers of possible combinations of cations and anions in dicationic ILs are greater than in monocationic ILs. Therefore, broader variability in the physical properties of these ILs should be possible such that changes in their structure can be "tuned", controlled or altered to a greater extent than conventional ILs.[3−5]

These DILs have been studied in different applications such as electrolytes,[6] additives in chromatography,[7] solvents for high-temperature organic reactions,[8] and agents for selectively complexing and extracting mercury(II).[9] There are several studies on the physical properties (e.g., density and viscosity) of DILs. Most of these properties are related to structural changes[6,10,11] rather than temperature changes, as is usually the case in monocationic ILs.

In this work, a new DIL with a functional amino group in the imidazolium ring and a bis(trifluoromethanesulfonyl)imide anion was synthesized. Metallic ions can be extracted from aqueous solution by a chelating effect by at least two points in the extracting agent structure, as occurs with a great variety of oxime compounds.[12,13] Due to their modified substituents this IL was designed for application in the liquid−liquid extraction of metal ions such as ferric and cupric ions in mineral processing in northern Chile.

Since this is a new compound, the knowledge of physical properties is of great importance for process engineering and equipment design, and thus, the density, dynamic viscosity, and refractive index were measured as a function of temperature from (298.15 to 343.15) K. The coefficient of thermal expansion was obtained from experimental density data as a function of temperature. Moreover, the standard entropy was calculated using the expression proposed by Glasser.[14] The Lorentz−Lorenz, Dale−Gladstone, Oster, Arago−Biot, Newton, Eykman, and modified Eykman empirical equations were used to evaluate the correlation between the densities and refractive indices of the IL. In addition, the thermal behavior of this new compound was determined with TGA and DSC analysis.

EXPERIMENTAL SECTION

Chemicals. For the synthesis, imidazole with a purity of > 99 %, acrylonitrile with a purity of > 99 %, 1,4-dibromobutane with a purity of > 99 %, 2-bromoacetamide with a purity of > 98 %, and lithium bis(trifluoromethanesulfonyl)imide with a purity of > 99 % were procured from Sigma-Aldrich and used without further purification. Milli-Q quality distilled water was used in all experiments ($\kappa = 0.054\ \mu S \cdot cm^{-1}$).

Synthesis. The new compound 1,1′-butane-1,4-di-yl-bis[3-(2-amino-2-oxoethyl)-1*H*-imidazol-3-ium] dibis-(trifluoromethanesulfonyl)imide ($[C_4(amim)_2]TFSI_2^-$) was synthesized as follows. Imidazole (15.49 g, 0.227 mol) was dissolved in methanol in a round-bottom flask placed in a heating jacket connected to a thermo-regulated Lauda RM-B bath, with an accuracy of ± 0.1 K. An excess of acrylonitrile (21.09 g, 0.397 mol) was added dropwise. The system was degassed several times with dry argon, heated at 333.15 K, and stirred for 6 h. Methanol and unreacted acrylonitrile were removed under reduced pressure, and the temperature was increased to 353.15 K, resulting in compound **A** (Figure 1). After cooling to 278.15 K, 2-bromoacetamide dissolved in acetonitrile was carefully added dropwise, and an exothermic reaction was observed. The

Received: December 20, 2011
Accepted: June 20, 2012

   dx.doi.org/10.1021/je3000876 | *J. Chem. Eng. Data* XXXX, XXX, XXX−XXX

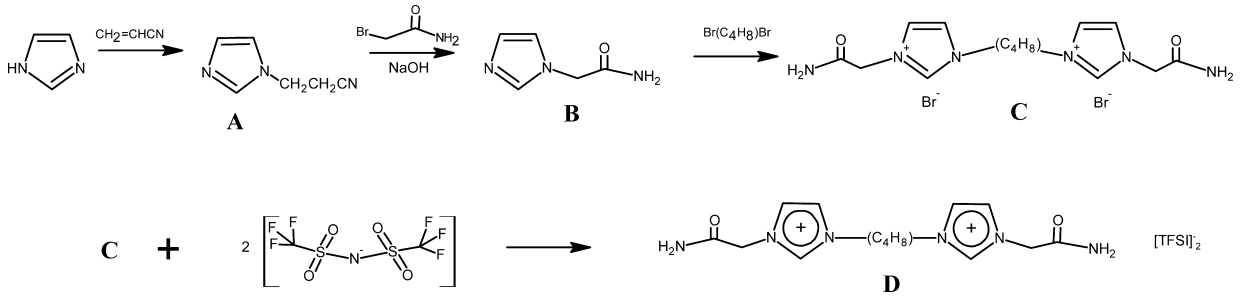

Figure 1. Route of synthesis of the DIL 1,1′-butane-1,4-di-yl-bis[3-(2-amino-2-oxoethyl)-1*H*-imidazol-3-ium] dibis(trifluoromethanesulfonyl)imide dibis(trifluoromethanesulfonyl)imide.

mixture was stirred for 13 h, increasing the temperature gradually until reaching 323.15 K. After the reaction was completed, an excess of 15 wt % NaOH and chloroform were added, and this mixture was left to stir at room temperature for 1 h, until an organic and aqueous phase was observed. The viscous brown upper phase was separated, and residual solvent was removed under reduced pressure at 353.15 K, yielding 27.53 g (0.22 mol) of compound **B** (Figure 1). Afterward, 1,4-dibromobutane (24.5 g, 0.11 mol) was added dropwise to the mixture of methanol and compound **B** under dry argon atmosphere, resulting in an homogeneous mixture that was left to stir at 323.15 K for 96 h under reflux. Methanol was removed under reduced pressure and heated to 353.15 K. The product **C** (Figure 1) was washed several times with 20 cm^3 of ethyl acetate to eliminate the unreacted reagents, and the remaining ethyl acetate (b.p.: 350 K) was removed under reduced pressure at 343.15 K. The bromide salt was finally dried in vacuo at 343.15 K. The obtained product was a very viscous light brown liquid (51.21 g, 0.11 mol, 93 % yield).

For the metathesis reaction, compound **C** (Figure 1) was dissolved in deionized water. The lithium bis(trifluoromethanesulfonyl)imide salt (66.8 g, 0.23 mol) was added and left to stir for 1 h at room temperature. Two liquid phases were observed; the bottom phase was washed several times with deionized water. The bromide salt in the residual water was detected with $AgNO_3$ 0.1 N. By the third wash, there was no presence of bromide salt. The product was dried in vacuo at 353.15 K. The water content was determined using a Karl Fischer titrator and was found to be 0.0034 mass fraction. The final obtained product **D** (Figure 1) was a very viscous yellow liquid. Yield 80.5 %. ^{1}H NMR (MeOD, δ ppm): 3.48 (m, 2H), 3.98 (t, 2H), 5.02 (s, 2H), 7.81 (s, 1H), 7.89 (s, 1H), 9.24 (s, 1H). FT-IR (400 to 4000 cm^{-1}). 3453, 3361 [υ(N−H)]. 3157, 2974 [υ(Ar−C−H)]. 1754, 1701 [υ(C═O)]. 1614, 1459 [υ(C═C)]. 1568 [$\upsilon(NH_2)$]. CHN analysis: % calcd, (% found): C 24.95 (26.30), H 2.56 (1.84), N 12.93 (11.91), S 14.80 (13.18).

Apparatus and Procedure. The water content has been determinate by a Karl Fischer titrator Mettler Toledo DL31, with an uncertainty of ± 0.0005 mass fraction (Combititrant 5, one component 1 mL = ca. 5 mg of H_2O). After drying, samples were stored under dry atmosphere in vacuum desiccators.

The physical properties were measured in triplicate at the specified temperature. The densities were measured with a Mettler Toledo DE-50 vibrating tube densimeter, with an uncertainty of less than ± $5{\cdot}10^{-2}$ kg·m^{-3}. The densimeter was calibrated at atmospheric pressure using air and distilled deionized water as a reference substance prior to the initiation of each run of measurements at a given temperature. The refractive index was measured using a Mettler Toledo RE50 refractometer with an uncertainty of ± $1{\cdot}10^{-4}$ n_D units. The densimeter and refractometer had self-contained Peltier systems for temperature control with an uncertainty of ± 0.1 K. Dynamic measurements of viscosity were implemented using a Brookfield model DV-III cone/planar rheometer with a CP-40 spindle. A Lauda model RM-6 water circulator bath was used to maintain the temperature of the measurements within ± 0.1 K. The average reproducibility of the viscosity measurements was ± 0.00125 Pa·s. All viscosity measurements were carried out at a constant share rate of 0.225 s^{-1}.

For the thermogravimetric analysis, a TGA/DSC-1 from Mettler Toledo was used. The instrument was calibrated for temperature and heat flow with an indium reference sample provided by Mettler Toledo. The measurement was repeated three times with an approximate mass of 13 mg, which was placed in a 70 μL alumina crucible with a lid and small hole, in the temperature range of (298.15 to 823.15) K at a heating rate of 10 K·min^{-1}. The Mettler Toledo STAR^e software version 10.0 was used to determine the onset and start temperature. The start temperature (T_{start}) is the temperature at which the decomposition of the sample begins. The onset temperature (T_{onset}) is the intersection of the baseline weight, either from the beginning of the experiment or after the drying step, and the tangent of the weight versus the temperature curve as decomposition occurs.

Differential scanning calorimetry (DSC) was performed using a Mettler Toledo DSC 821 calorimetric system using the STAR^e program. Dry nitrogen was used as a purge gas and measured in the temperature range of (120.18 to 360.18) K at a scan rate of 20 K·min^{-1}.

RESULTS AND DISCUSSION

The physical properties were measured experimentally from (298.15 to 343.15) K at atmospheric pressure using the above-mentioned techniques and are shown in Table 1.

The density of the DIL was found to be denser than most monocationic ILs and similar to other DILs with short alkyl chains as a spacer between cations.[10] As expected, the density of the IL decreased with an increase in temperature, which is usually the case for other ILs.[15−17] The variation in density with respect to temperature for the IL is illustrated in Figure 2. The density values were fitted using the following quadratic equation:

$$\rho = A_0 + A_1 T + A_2 T^2 \quad (1)$$

where T is the absolute temperature and A_0, A_1, and A_2 are adjustable parameters. These correlation parameters and the standard relative deviations (SRDs) are given in Table 2.

Density data were used to derive other thermodynamic properties, such as the thermal expansion coefficient. This

dx.doi.org/10.1021/je3000876 | J. Chem. Eng. Data XXXX, XXX, XXX−XXX

Table 1. Density, ρ, Refractive Index, n_D, Thermal Expansion Coefficient, α, and Dynamic Viscosity, η, as a Function of Temperature

T/K	ρ/kg·m^{-3}	α/K^{-1}	n_D	η/Pa·s
298.15	1590.17	0.00057	1.4546	8.689
303.15	1585.41	0.00057	1.4532	4.730
308.15	1580.62	0.00058	1.4518	3.285
313.15	1575.98	0.00059	1.4504	2.365
318.15	1572.04	0.00059	1.4491	1.824
323.15	1567.22	0.00060	1.4477	1.517
328.15	1562.31	0.00060	1.4464	1.323
333.15	1557.66	0.00061	1.4451	1.221
338.15	1552.61	0.00062	1.4439	1.129
343.15	1548.03	0.00062	1.4430	1.098

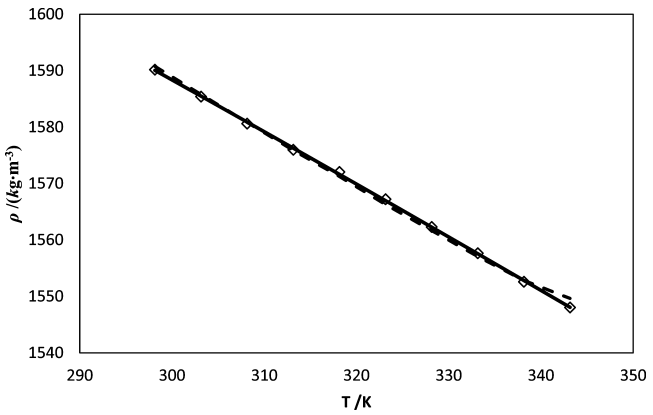

Figure 2. Plot of density, ρ, against temperature, T, and fitted curves.

Table 2. Fitting Parameters and Standard Deviations for Correlating Density and Refractive Index as a Function of Temperature

physical properties	A_0	A_1	A_2	SRD[a]
ρ/(kg·m^{-3})	1820.99	−0.6369	−0.0005	0.2179
n_D	1.6150	$-7.8\cdot10^{-4}$	$8.03\cdot10^{-7}$	0.0001

[a]Calculated with eq 7.

coefficient is related to the temperature derivative of the density through the following equation:[18]

$$\alpha = \frac{1}{V}\left(\frac{\partial V}{\partial T}\right)_p = -\frac{1}{\rho}\left(\frac{\partial \rho}{\partial T}\right)_p \quad (2)$$

where α is the coefficient of thermal expansion, V is the molar volume of the IL, ρ is the DIL density, and $(\partial\rho/\partial T)_p$ is the value $A_1 + 2A_2\cdot T$ using A_1 and A_2 parameters from the fitting of eq 1. The thermal expansion coefficient is shown in Table 1. It slightly increases with temperature and varies between ($5.4\cdot10^{-4}$ and $6.2\cdot10^{-4}$) K^{-1}. The change in these values is smaller than the estimated uncertainty, and it can thus be considered to be independent of the temperature. Recently, Navia et al.[19] have presented experimental data on thermal expansion with the most widely studied ILs. They compared the experimental data obtained with calculated data from eq 2 and found deviations within the accepted limits after taking into account the uncertainty of the measured density data and the fitting equation. To some extent, these results can corroborate that this method is valid for the calculation of α of ILs. Moreover, the value obtained here is within the common range for ILs reported in the literature[20−23] ranging from ($5\cdot10^{-4}$ to $7.7\cdot10^{-4}$) K, which is lower than the value of α typical for conventional molecular solvents.

From the experimental densities, the IL molecular volume (V_{molec}) was calculated at T = 298.15 K using the following equation:[17,24]

$$V_{molec}/\mathrm{nm}^3 = \frac{M}{N\cdot\rho} \quad (3)$$

where M is the molar mass (866.65 g·mol^{-1}), and N is Avogadro's number. The value obtained from this equation is 0.9049 nm^3.

Glasser and Jenkins[25,26] have established a linear relationship between entropy (S^0) and the molecular volume for ionic solids and organic solids. These equations have been adapted for ILs.[14,17,24] Since ILs with large organic cations are defined between ionic solids and organic liquids, the average values of the linear correlation constants are used:

$$S^0/(\mathrm{J\cdot K^{-1}\cdot mol^{-1}}) = 1246.58(V_{molec}/\mathrm{nm}^3) + 29.5 \quad (4)$$

Thus, $S^0/(\mathrm{J\cdot K^{-1}\cdot mol^{-1}}) = 1157.5$.

As expected, the viscosity of the DIL showed a marked decrease with increasing temperature. The variation in the viscosity with temperature for the IL studied here is illustrated in

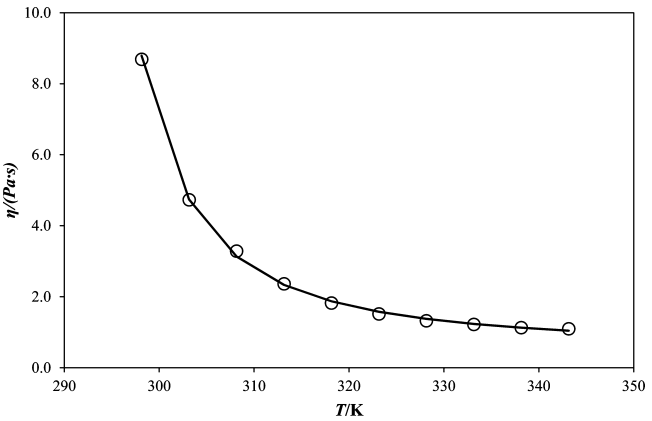

Figure 3. Plot of dynamic viscosity, η, against temperature, T, and curve fitted with the VTF equation: ○, experimental data; —, calculated eq 6.

Figure 3. The viscosity data were fitted using an Arrhenius-like law:

$$\eta = \eta_\infty \exp\left(-\frac{E_a}{RT}\right) \quad (5)$$

where R is the universal gas constant and the characteristic parameters are viscosity at infinite temperature (η_∞) and activation energy (E_a). However, for ILs, it has been reported[20,21,27] that a better description is provided by the modified version of the Vogel−Fulcher−Tammann (VTF) equation that characterizes glass-forming liquids:

$$\eta = AT^{0.5} \exp\left(\frac{B}{T - T_0}\right) \quad (6)$$

where A, B, and T_0 are adjustable parameters. Table 3 lists the parameters for both equations obtained using the standard relative deviation (SRD):

dx.doi.org/10.1021/je3000876 | J. Chem. Eng. Data XXXX, XXX, XXX−XXX

Table 3. Adjustable Parameters of the Arrhenius and VTF Equations with Fit Deviation with Respect to Viscosity

	A	B	T_0	η_∞	E_a	
equation	Pa·s·K	K	K	Pa·s	kJ·mol^{-1}	SRD
VTF	$2.06\cdot10^{-2}$	66	278			0.0359
Arrhenius				$3.61\cdot10^{-1}0$	−59.3	0.8299

$$\mathrm{SRD} = \left\{ \sum_i^{\eta_\infty} \left(\frac{z_{\mathrm{exp}} - z_{\mathrm{cal}}}{z_{\mathrm{cal}}} \right)^2 / (n_{\mathrm{dat}} - n_{\mathrm{p}}) \right\}^{1/2} \quad (7)$$

where z_{exp} and z_{cal} are the values of the experimental calculated property, n_{dat} is the number of experimental data points, and n_p is the number of parameters.

It is clear that the VTF model provides a better fit, and the correlated values are in good agreement with the experimental data. This result was expected because the VTF model contains three parameters compared to two for the Arrhenius equation.

The refractive index data n_D were fitted using the following equation:

$$n_{\mathrm{D}} = A_0 + A_1 T + A_2 T^2 \quad (8)$$

where T is the absolute temperature, and A_0, A_1, and A_2 are adjustable parameters, which are shown in Table 2 together with the standard deviation. Variation as a function of temperature and the fitting results are illustrated in Figure 4, and a decrease is clearly observed when the temperature is increased.

The experimental refractive index was used to correlate the experimental density using several empirical equations of the following form:

$$f(n_{\mathrm{D}}) = k\rho = \begin{cases} \dfrac{{n_{\mathrm{D}}}^2 - 1}{{n_{\mathrm{D}}}^2} & \text{(Lorentz–Lorenz)} \\ n_{\mathrm{D}} - 1 & \text{(Dale–Gladstone)} \\ \dfrac{{n_{\mathrm{D}}}^2 - 1}{n_{\mathrm{D}} + 0.4} & \text{(Eykman)} \\ \dfrac{({n_{\mathrm{D}}}^2 - 1)(2{n_{\mathrm{D}}}^2 + 1)}{{n_{\mathrm{D}}}^2} & \text{(Oster)} \\ n_{\mathrm{D}} & \text{(Arago–Biot)} \\ {n_{\mathrm{D}}}^2 & \text{(Newton)} \\ \dfrac{{n_{\mathrm{D}}}^2 - 1}{n_{\mathrm{D}} + d} & \text{(Eykman modified)} \end{cases}$$

where $f(n_D)$ is a function of refractive index, such as in the Lorentz–Lorenz, Dale–Gladstone, Eykman, Oster, Arago–Biot and Newton equations. In these equations, k is an empirical constant that depends on the liquid and the wavelength at which the refractive index is measured. In this study, the modified Eykman equation proposed by Pineiro et al.[28] is tested by taking into account the optimization of the new parameter d.

The parameters k and d along with the standard deviation from the mathematical fittings are shown in Table 4. Based on these results, the modified Eykman equation shows the best fit with the experimental data; this was expected because the modified Eykman equation uses two parameters, while the other equations use only one. Among the one-parameter equations, the Dale–Gladstone and Oster equations show the best results.

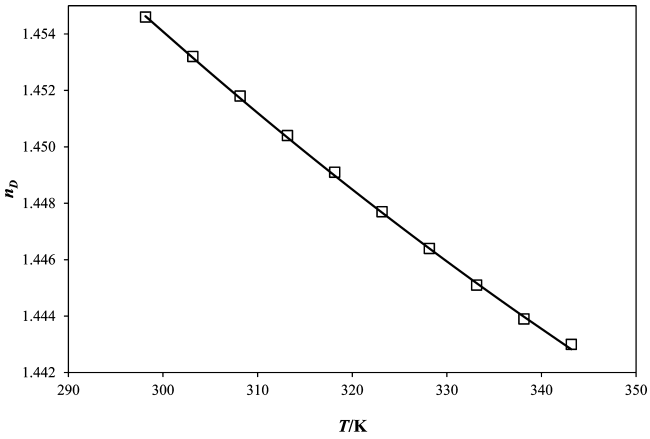

Figure 4. Refractive index plotted against temperature and the fitted curve: □, experimental data; —, calculated eq 8.

Table 4. Fitting Parameters and Standard Deviations for Deriving Density Using Refractive Index Data

	k	d	SD*
Eykman modified	0.0003	1.1900	0.7327
Dale–Gladstone	0.0003		0.7550
Oster	0.0017		0.9908
Eykman	0.0004		1.2136
Lorentz–Lorenz	0.0002		2.0822
Newton	0.0013		5.2597
Arago–Biot	0.0009		9.3220

*SD = $(\sum i_{\mathrm{DAT}}^{n}(z_{\mathrm{exp}} - z_{\mathrm{adjust}})^2/n_{\mathrm{DAT}})^{0.5}$, where n_{DAT} is the number of the experimental data.

Figure 2 shows the results of the density calculations from refractive index data using the modified Eykman equation together with correlated data using eq 2. As shown in this figure, the density correlation with the refractive index data fits well with the present measurements, as does eq 2. Furthermore, this correlation for density calculation using the refractive index measurements could be very helpful because the refractive index measurements are much simpler than the density measurements.

The thermal stability of the IL is shown in Figure 5. At first sight, the thermal stability seems to be above 650 K (dotted line);

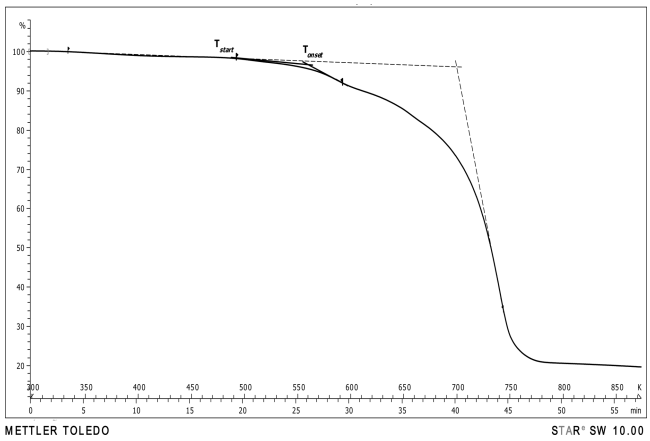

Figure 5. TGA results for the IL.

dx.doi.org/10.1021/je3000876 | J. Chem. Eng. Data XXXX, XXX, XXX–XXX

however, a detailed observation reveals a decrease in the weight at 558.1 K, which levels off approximately 615 K and then is followed by an abrupt decrease above 650 K. These temperatures are the start temperature, determined from the step tangent[29] where the start point of decomposition can be stated at 558.1 K (T_{onset}). Thermal decomposition is strongly dependent on the IL structure, but it also depends on the crucible material and the sample mass.[30] In addition, the IL does not completely evaporate, since an amount of charcoal in the crucible was observed after the measurement, as has been observed in other studies with ILs.[30] The decomposition of imidazolium salts is attributed to decomposition of the cation, which is facilitated by the anion, while pyrolysis of imidazolium salts yielded volatile degradation products such as 1-alkylimidazoles.[31]

The DSC thermogram obtained at a rate of 20 K·min^{-1} is shown in Figure 6. The heat jump observed is the calorimetric

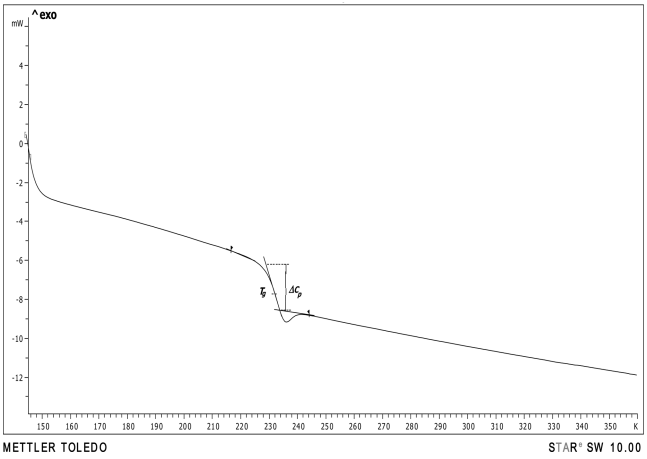

Figure 6. DSC scan for the IL showing the glass transition.

fingerprint of the glass transition at temperature T_g = 230.5 K; this value shows that the glass transition temperature is low, and it is in line with other reported $[TFSI_2]^-$ anion-based DILs with functional groups in the cation substituent, which have a value of 250 K.[32] In addition, the glass transition temperatures of dicationic ILs are generally higher than those of monocationic $[TFSI_2]^-$ anion and imidazolium cation-based ILs, which are in the range of (218 to 183) K. On the other hand the results show that, in the temperature range used for the measurements, there was no crystallization during cooling, and therefore, no melting point was observed. This behavior has also been noted with other dicationic[32] and monocationic[33] ILs. This is probably because the flexible structure of the $[TFSI_2]^-$ anion makes it difficult to crystallize.[34]

The sigmoidal change in the heat flux, which is characteristic of the glass transition on DSC, is caused from a change in heat capacity (ΔC_p) when the sample is heated from the glassy state to a metastable supercooled liquid.[35] In this case, ΔC_p= 311.8 J·mol^{-1}·K^{-1}. This high heat capacity jump at the glass transition appears to be a specific feature of ILs. The high value of ΔC_p in the T_g found for ILs is related to the fact that each molecular unit is actually composed of two subunits (i.e., the cation and anion), which, in the liquid state, have appreciable relative mobility.

CONCLUSIONS

A new functionalized dicationic IL was prepared, and the density, dynamic viscosity, and refractive index of the IL were measured in a temperature range of (298.15 to 343.15) K. In addition, results from thermal stability analysis and DSC scanning were presented. In general, all experimental physical properties exhibited a decrease with an increase in temperature in the range of temperature studied. Empirical equations were used to fit the experimental data of the measured physical properties, resulting in good agreement. Density data were used to derive the thermal expansion coefficient, and the molecular volume and standard entropy of the IL were calculated at T = 298.15 K. Several empirical equations were used to fit the experimental density data using the refractive index data. Good agreement was found with the modified Eykman equation; this finding can be useful for deriving approximate density data. Thermal stability was established at 558.1 K. Based on the DSC scan, no melting point was found, and the glass transition temperature was 230.5 K, with ΔC_p = 311.8 J·mol^{-1}·K^{-1}.

AUTHOR INFORMATION

Corresponding Author

*E-mail: tgraber@uantof.cl.

Funding

The authors acknowledge Conicyt-Chile for their support provided through the project Fondecyt 1085059. M.C. also thanks Conicyt-Chile for a doctoral fellowship.

Notes

The authors declare no competing financial interest.

REFERENCES

(1) Wasserscheid, P.; Welton, T. *Ionic Liquids in synthesis*, 2nd ed.; Wiley-VCH Verlag GmbH & Co. KGaA.: 2008; Vol. *1*.

(2) Seddon, K. R.; Rogers, R. D. *Ionic liquids: industrial applications for green chemistry*; American Chemical Society: Washington, DC, 2002.

(3) Payagala, T.; Huang, J.; Breitbach, Z. S.; Sharma, P. S.; Armstrong, D. W. Unsymmetrical dicationic ionic liquids: manipulation of physicochemical properties using specific structural architectures. *Chem. Mater.* **2007**, *19* (24), 5848−5850.

(4) Liu, X.; Xiao, L.; Wu, H.; Chen, J.; Xia, C. Synthesis of Novel Gemini Dicationic Acidic Ionic Liquids and Their Catalytic Performances in the Beckmann Rearrangement. *Helv. Chim. Acta* **2009**, *92* (5), 1014−1021.

(5) Chang, J. C.; Ho, W. Y.; Sun, I. Synthesis and characterization of dicationic ionic liquids that contain both hydrophilic and hydrophobic anions. *Tetrahedron* **2010**, *66* (32), 6150−6155.

(6) Zhang, Z.; Yang, L.; Luo, S.; Tian, M.; Tachibana, K.; Kamijima, K. Ionic liquids based on aliphatic tetraalkylammonium dications and TFSI anion as potential electrolytes. *J. Power Sources* **2007**, *167* (1), 217−222.

(7) Huang, K.; Han, X.; Zhang, X.; Armstrong, D. W. PEG-linked geminal dicationic ionic liquids as selective, high-stability gas chromatographic stationary phases. *Anal. Bioanal. Chem.* **2007**, *389* (7), 2265−2275.

(8) Han, X.; Armstrong, D. W. Using geminal dicationic ionic liquids as solvents for high-temperature organic reactions. *Org. Lett.* **2005**, *7* (19), 4205−4208.

(9) Holbrey, J. D.; Visser, A. E.; Spear, S. K.; Reichert, W. M.; Swatloski, R. P.; Broker, G. A.; Rogers, R. D. Mercury (II) partitioning from aqueous solutions with a new, hydrophobic ethylene-glycol functionalized bis-imidazolium ionic liquid. *Green Chem.* **2003**, *5* (2), 129−135.

(10) Anderson, J. L.; Ding, R.; Ellern, A.; Armstrong, D. W. Structure and properties of high stability geminal dicationic ionic liquids. *J. Am. Chem. Soc.* **2005**, *127* (2), 593−604.

(11) Zeng, Z.; Phillips, B. S.; Xiao, J. C.; Shreeve, J. M. Polyfluoroalkyl, polyethylene glycol, 1,4-bismethylenebenzene, or 1,4-bismethylene-2,3,5,6-tetrafluorobenzene bridged functionalized dicationic ionic liquids: synthesis and properties as high temperature lubricants. *Chem. Mater.* **2008**, *20* (8), 2719−2726.

(12) Domic, E. *Hidrometalurgia: Fundamentos*; Procesos y Aplicaciones: Santiago-Chile, 2001.
(13) *MCTRedbook: Solvent Extraction Reagents and Applications*; Cognis-Group: North Rhine, Germany, 2008.
(14) Glasser, L. Lattice and phase transition thermodynamics of ionic liquids. *Thermochim. Acta* **2004**, *421* (1−2), 87−93.
(15) Soriano, A. N.; Doma, B. T., Jr.; Li, M. H. Density and refractive index measurements of 1-ethyl-3-methylimidazolium-based ionic liquids. *J. Taiwan Inst. Chem. Eng.* **2010**, *41* (1), 115−121.
(16) Gardas, R. L.; Ge, R.; Goodrich, P.; Hardacre, C.; Hussain, A.; Rooney, D. W. Thermophysical Properties of Amino Acid-Based Ionic Liquids. *J. Chem. Eng. Data* **2009**, *55* (4), 1505−1515.
(17) Deive, F. J.; Rivas, M. A.; Rodríguez, A. Thermophysical properties of two ionic liquids based on benzyl imidazolium cation. *J. Chem. Thermodyn.* **2011**, *43* (3), 487−491.
(18) Smith, J. M.; Van Ness, H.; Abbott, M. *Introduction to Chemical Engineering Thermodynamics*, 6th ed.; McGraw-Hill: New York, 2001.
(19) Navia, P.; Troncoso, J.; Romaní, L. Dependence against Temperature and Pressure of the Isobaric Thermal Expansivity of Room Temperature Ionic Liquids. *J. Chem. Eng. Data* **2009**, *55* (2), 595−599.
(20) Gómez, E.; González, B.; Calvar, N.; Tojo, E.; Domínguez, Á. Physical properties of pure 1-ethyl-3-methylimidazolium ethylsulfate and its binary mixtures with ethanol and water at several temperatures. *J. Chem. Eng. Data* **2006**, *51* (6), 2096−2102.
(21) Rodríguez, H.; Brennecke, J. F. Temperature and composition dependence of the density and viscosity of binary mixtures of water + ionic liquid. *J. Chem. Eng. Data* **2006**, *51* (6), 2145−2155.
(22) Zang, S.; Fang, D. W.; Li, J.; Zhang, Y. Y.; Yue, S. Estimation of Physicochemical Properties of Ionic Liquid HPReO4 Using Surface Tension and Density. *J. Chem. Eng. Data* **2009**, *54* (9), 2498−2500.
(23) Li, J.-G.; Hu, Y.-F.; Ling, S.; Zhang, J.-Z. Physicochemical Properties of [C6mim][PF6] and [C6mim][(C2F5)3PF3] Ionic Liquids. *J. Chem. Eng. Data* **2011**, *56* (7), 3068−3072.
(24) Pereiro, A. B.; Veiga, H. I. M.; Esperança, J. M. S. S.; Rodríguez, A. Effect of temperature on the physical properties of two ionic liquids. *J. Chem. Thermodyn.* **2009**, *41* (12), 1419−1423.
(25) Glasser, L.; Jenkins, H. D. B. Standard absolute entropies, S°298, from volume or density: Part II. Organic liquids and solids. *Thermochim. Acta* **2004**, *414* (2), 125−130.
(26) Glasser, L.; Jenkins, H. D. B. Predictive thermodynamics for condensed phases. *Chem. Soc. Rev.* **2005**, *34* (10), 866−874.
(27) Fernández, A.; García, J.; Torrecilla, J. S.; Oliet, M.; Rodríguez, F. Volumetric, Transport and Surface Properties of [bmim][$MeSO_4$] and [emim][$EtSO_4$] Ionic Liquids As a Function of Temperature. *J. Chem. Eng. Data* **2008**, *53* (7), 1518−1522.
(28) Piñeiro, Á.; Brocos, P.; Amigo, A.; Pintos, M.; Bravo, R. Surface tensions and refractive indices of (tetrahydrofuran + n-alkanes) at T = 298.15 K. *J. Chem. Thermodyn.* **1999**, *31* (7), 931−942.
(29) Ngo, H. L.; LeCompte, K.; Hargens, L.; McEwen, A. B. Thermal properties of imidazolium ionic liquids. *Thermochim. Acta* **2000**, *357*, 97−102.
(30) Kosmulski, M.; Gustafsson, J.; Rosenholm, J. B. Thermal stability of low temperature ionic liquids revisted. *Thermochim. Acta* **2004**, *412*, 47−53.
(31) Kamavaram, V.; Reddy, R. G. Thermal stabilities of di-alkylimidazolium chloride ionic liquids. *Int. J. Therm. Sci.* **2008**, *47* (6), 773−777.
(32) Pitawala, J.; Matic, A.; Martinelli, A.; Jacobsson, P.; Koch, V.; Croce, F. Thermal Properties and Ionic Conductivity of Imidazolium Bis(trifluoromethanesulfonyl) imide Dicationic Ionic Liquids. *J. Phys. Chem. B* **2009**, *113* (31), 10607−10610.
(33) Fredlake, C. P.; Crosthwaite, J. M.; Hert, D. G.; Aki, S. N. V. K.; Brennecke, J. F. Thermophysical properties of imidazolium-based ionic liquids. *J. Chem. Eng. Data* **2004**, *49* (4), 954−964.
(34) Shirota, H.; Mandai, T.; Fukazawa, H.; Kato, T. Comparison between Dicationic and Monocationic Ionic Liquids: Liquid Density, Thermal Properties, Surface Tension, and Shear Viscosity. *J. Chem. Eng. Data* **2011**, *56* (5), 2453−2459.
(35) Moura Ramos, J. J.; Alfonso, C. A. M.; Branco, L. C. Glass transition relaxation and fragility in two room temperature ionic liquids. *J. Therm. Anal. Calorim.* **2003**, *71* (2), 656−666.